

See discussions, stats, and author profiles for this publication at: <https://www.researchgate.net/publication/228813039>

Real-Time Probing of Intramolecular Vibrational Energy Redistribution and Intermolecular Vibrational Energy Transfer of Selectively Excited CH₂I₂ Molecules in Solution †

ARTICLE *in* THE JOURNAL OF PHYSICAL CHEMISTRY A · MAY 2001

Impact Factor: 2.69 · DOI: 10.1021/jp004293u

CITATIONS

46

READS

41

4 AUTHORS, INCLUDING:



Bernd Abel

Leibniz Institute of Surface Modification

137 PUBLICATIONS 1,962 CITATIONS

SEE PROFILE

Real-Time Probing of Intramolecular Vibrational Energy Redistribution and Intermolecular Vibrational Energy Transfer of Selectively Excited CH₂I₂ Molecules in Solution[†]

Ales Charvat, Jens Aßmann, and Bernd Abel*

Institut für Physikalische Chemie, Universität Göttingen, Tammannstrasse 6, 37077 Göttingen, Germany

Dirk Schwarzer

Max-Planck Institut für biophysikalische Chemie, Am Fassberg 10, 37077 Göttingen, Germany

Received: November 28, 2000; In Final Form: March 12, 2001

Competition between intramolecular vibrational energy redistribution (IVR) and intermolecular vibrational energy transfer (VET) of excited methylene iodide (CH₂I₂) in solution has been measured in real time. After excitation of the C–H– stretch overtone and C–H– stretch containing combination bands of CH₂I₂ between 1.7 and 2.4 μm an increase followed by a decrease in the transient electronic absorption at 400 nm has been monitored. The transient absorption has been attributed to vibrational energy flow from the initially excited degrees of freedom to vibrational states with larger Franck-Condon (FC) factors for the electronic transition (long wavelength wing) and energy loss due to energy transfer to the solvent. A model based upon the dependence of the electronic absorption on the internal energy $\langle E \rangle$ of CH₂I₂ has been used to determine the times for intramolecular vibrational energy redistribution and intermolecular energy transfer to the solvent. In the simplest version of our model the internal energy of the molecule probed by the population of the FC-active modes rises and decays exponentially on a picosecond (ps) time scale, which reflects the initial intramolecular vibrational energy redistribution and the subsequent energy transfer to the solvent. This simple approach was able to accurately describe the measured transient absorption for all solvents and excitation wavelengths. Overall time constants for IVR have been found to be on the order of 9–10 ps, almost independent of the excitation wavelength, the excited modes, and the solvent. In contrast, energy transfer to the solvent takes significantly longer. Overall time constants for VET have been determined in the range between 60 and 120 ps depending on the solvent, the excitation energy, but not on the mode which was initially excited.

I. Introduction

Knowledge about the competition and the time scales of intramolecular vibrational energy redistribution (IVR) and intermolecular vibrational energy transfer (VET) of selectively vibrationally excited molecules in solution on a molecular level is essential for the understanding of rates, pathways, and efficiencies of chemical transformations in solution.^{1–3} Although, we have witnessed enormous theoretical efforts^{2–12} and progress in computational power in the past decade, theory is still far from being able to quantitatively explain detailed IVR and VET experiments in solution or to have predictive power for realistic systems. Therefore, detailed experiments are often needed to guide theory and to develop theoretical models.

In the case of large organic molecules several experiments have been reported in which VET of highly excited molecules after internal conversion could be measured (azulene,^{13–16} stilbene,^{17–21} anthracene,²² dye molecules^{23–26}). With Raman techniques (e.g., Stokes²⁷ and anti-Stokes Raman scattering^{1,28–30}), infrared saturation,³¹ and pump-and-probe spectroscopy,³² IVR and VET of mid-sized halocarbons,^{29,31–37} water,³² alcohols,^{30,38,39} nitromethane,⁴⁰ benzene,⁴¹ acetonitrile^{40,42} has been studied in considerable detail. CH₂I₂, like other halocarbons above, has been the subject of several studies as well.^{31,37,43} However, most of the vibrationally selective experimental

techniques employed to date have only been used to investigate inter- and intramolecular dynamics in the energy region of the fundamentals. Although, there are a few exceptions there is clearly the need for direct sensitive techniques to measure the energy (and mode) dependence of IVR and VET in (high) overtones of molecules in solution.

In the present work we used a mode-specific experimental approach, recently developed by Crim et al.,³⁷ employing near-infrared (IR) and near-ultraviolet (UV) femtosecond-laser pulses for the direct measurement of IVR and VET in the liquid phase. The present experiments are an extension of their recent studies on CH₂I₂. The new features of the present approach are the measurement of the energy and mode dependence of IVR and VET and the conversion of the absorption data into internal energies via high-temperature shock tube data.

II. Experiment

A. Experimental Approach. Our IR excitation and near UV probe technique makes use of mode-selective near-infrared excitation of overtones and combination bands and subsequent detection of the enhancement of electronic absorption. This approach closely resembles vibrationally mediated photodissociation in the gas phase pioneered by the Crim group^{44–46} and is an extension of their scheme that has been used to follow intramolecular energy redistribution in gases⁴⁶ and in liquids.³⁷ In an electronic absorption, in general, only a few modes are FC-active, which can be identified in resonance Raman experi-

* Corresponding author. E-mail: Babel@gwdg.de.

[†] Dedicated to Prof. Dr. J. Troe on the occasion of his 60th birthday.

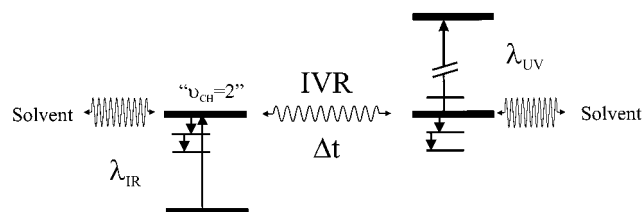


Figure 1. Experimental scheme. In our pump-and-probe experiment the first near-IR femtosecond-laser pulse prepares a vibrationally excited molecule with an energy of 4000–6000 cm^{-1} in its ground electronic state, and a second laser pulse, tuned to the red wing of the electronic transition in the UV, measures the change in absorption induced by the first laser pulse.

ments. In the case of CH_2I_2 the resonance Raman spectra exhibit most of their intensity in fundamentals, overtones, and combination bands of modes nominally assigned to the C–I asymmetric stretch and to a minor degree to the I–C–I bend.^{47,48} The photodissociation coordinate in our vibrationally mediated photodissociation therefore appears to project primarily onto the asymmetric C–I stretching coordinate and to a minor degree onto the bending coordinate in the electronic ground state.^{37,47,48} For these reasons the present technique can be regarded to be a femtosecond-double-resonance technique, in principle, with mode-selective pump and probe. As shown schematically in Figure 1, in our pump and probe scheme the first near-IR femtosecond-laser pulse prepares a vibrationally excited molecule with an energy of 4000–6000 cm^{-1} in its ground electronic state, and a second laser pulse, tuned to the red wing of the electronic transition in the UV, measures the change in absorption induced by the first laser pulse. The transient change in electronic absorption is a direct consequence of the intramolecular equilibration and the subsequent energy loss due to VET to the solvent. Figure 1 schematically illustrates the pump and probe scheme and the evolution of vibrational energy.

The vibrational overtone excitation initially prepares some zeroth-order bright state corresponding to the first overtone of the C–H symmetric stretch vibration ($\nu_{\text{CH}} = 2$) or another lower energy combination vibration but does not immediately change the electronic absorption because the C–H stretch mode is FC-inactive. The total vibrational density of states in this case is on the order of 3–16 cm^{-1} , depending on the excited mode(s) and the considered energy range. Because the initially excited nonstationary state is not an eigenstate of the molecular Hamiltonian of the molecule in solution it evolves in time and vibrational energy flows from the C–H bond to other degrees of freedom including the FC-active modes which were not excited initially. As mentioned above these have been identified in recent resonance Raman experiments.^{47,48} Their increasing population enhances absorption of a time-delayed probe pulse tuned to the long wavelength wing of the electronic absorption spectrum. At the same time VET from the populated states of the molecules to the solvent takes place. Similar to the interpretation of Crim et al. we attribute the rise of the signal to intramolecular energy redistribution “populating” FC-active intramolecular modes and we identify a decaying signal with overall energy loss of the molecule and population moving out of these modes. Varying the time delay between the vibrational overtone excitation laser and the photolysis laser pulses allows us to directly observe the times for intramolecular vibrational energy redistribution, i.e., the time for energy to flow out of the initially excited nonstationary state into other degrees of freedom until a microcanonical ensemble is established (note that the absorption will change even in an isolated molecule until the energy is redistributed and FC-active modes are

populated statistically), and overall times for the energy transfer to solvent molecules. We make here use of the fact that canonical and microcanonical ensembles of molecules exhibit very similar UV spectra^{49,50} which depend sensitively on the population of only a few FC-active modes in the molecule and which can be used for probing the energy content in the molecule and progress in the evolution of an initially excited nonstationary state (with no excitation in FC-active modes) toward microcanonical and thermal equilibrium. In a simple picture we may think of Franck-Condon active modes as a local probe for the evolution of energy in the molecule and for the subsequent energy loss due to VET.^{49,50} To use UV absorptions of highly excited molecules as a measure for their internal energy the temperature dependence the spectra have to be measured accurately up to very high temperatures. Under the assumption that UV spectra of molecules in weakly interacting solvents are close to the corresponding gas-phase spectra we use the temperature-dependent spectra of CH_2I_2 measured in shock waves.

B. Experimental Technique. We generated the two laser pulses from a home-built regeneratively amplified (RGA) Ti:sapphire laser system. Transform-limited 15 fs pulses at a repetition rate of 96 MHz were obtained from the Kerr-lens mode-locked Ti:sapphire oscillator pumped by a Nd:YVO₄ laser at 532 nm (Coherent, Verdi). These pulses were stretched and then injected in the cavity of the regenerative amplifier (RGA). The RGA was pumped with a frequency-doubled Nd:YAG laser (Clark-MXR, ORC-1000) at 1 kHz. After amplification and compression 45–50 fs pulses with typical pulse energies of 0.6 mJ at 800 nm have been obtained. 400 μJ of the RGA was used to pump a commercial optical parametric amplifier based upon travelling wave optical parametric amplification of superfluorescence (TOPAS, Light Conversion) which generated the near-IR laser pulses at 1.6–2.5 μm which were used in the experiments (pulse width: ~ 50 fs, bandwidth: ~ 300 cm^{-1} at $\lambda = 1700$ nm). The remaining 200 μJ of the RGA output were doubled in a 200 μm BBO crystal providing probe pulse power at 400 nm well above 20 μJ . The delayed probe and the excitation pulse are attenuated, focused ($f = 200$ mm) and overlapped in a non collinear geometry (~ 5 deg.) in a thin (500 μm) quartz flow cell containing the liquid sample (1–2 M of CH_2I_2 in different solvents). The relative polarizations of the pump and probe pulses were set perpendicular to each other or at magic angle (54.7 deg.) in order to either minimize coherent artifacts or avoid signal from rotational relaxation. We measured transient absorption differences up to $\Delta\text{OD} = 1 \times 10^{-3}$ (ΔOD , change in optical density) on alternating shots at 1 kHz repetition rate and averaged up to 8×2000 shots after digitizing the signals in a microcomputer equipped with a fast AD converter (Data Translation). Measurements at different concentrations (0.5–2 M) did not provide evidence for contributions from solute interactions in the time-resolved traces. CH_2I_2 used in the present experiments had a specified purity of 98% (Aldrich) and was used without further purification. The solvents were obtained from Fluka.

III. Experimental Results and Data Analysis

A. Temperature-Dependent Spectra of CH_2I_2 . In general, the long wavelength absorption of electronic spectra is dominated by molecules with significant thermal energy. For example, Figure 2 displays the electronic absorption spectrum of CH_2I_2 in CCl_4 with a maximum around 290 nm and a weak long wavelength absorption between 300 nm and 420 nm. This hot band absorption in the long wavelength region of the

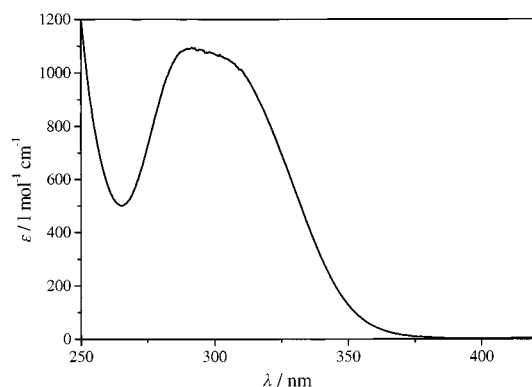


Figure 2. Absorption spectrum of CH₂I₂ in the range between 250 and 400 nm.

spectrum has a strong dependence on temperature. In general, the spectrum decays nearly exponentially in the red wing of the main absorption band. In addition, logarithm plots of the absorption coefficients at a particular wavelength on the red wing of the electronic absorption often tend to vary linearly with $1/T$ ($\log(\epsilon)$ vs $1/T$ plot), at least over small temperature intervals. Note, in this paper we use the expression “absorption coefficient” for ϵ , which is actually a molar extinction coefficient. The standard way of obtaining spectra of highly excited molecules (such as the molecules after near-IR excitation studied in this work) is to measure the temperature dependence of the spectra of the molecules in solution at a few temperatures near 300 K and to extrapolate the logarithm of the absorption cross section linearly vs $1/T$ toward very high temperatures.³⁷ Such a procedure, however, may be quite unreliable, because spectra of highly excited molecules may be very different than predicted from the temperature dependence close to 300 K. Although, theoretical predictions of the temperature dependence of UV spectra are qualitatively correct in general, the lack of precise information on electronically excited states in most cases still prevents quantitative predictions. Instead they have to be measured accurately in order to serve as a calibration for the internal energy and the distribution of internal energy in the molecule. Therefore, we have measured the temperature-dependent spectra between 276 and 315 K in CCl₄ (and other solvents with a very weak dependence on the solvents used in this study) and between 650 K and 1450 K in shock tube experiments. Since UV spectra of CH₂I₂ are not influenced by the presence of a nonpolar solvent they are quite similar to the corresponding spectra in the gas phase. This allows us to combine both sets of data and obtain the temperature-dependent absorption coefficient $\epsilon(T)$ and the dependence of the absorption coefficient on internal energy $\epsilon(\langle E \rangle)$ of the molecule at 400 nm (calculated from the temperature dependence of the internal energy). Both are plotted in Figure 3 and Figure 4. Also shown is a polynomial fit to the data to have a convenient analytical expression for $\epsilon(T)$ and $\epsilon(\langle E \rangle)$. It is very obvious from Figure 3 that a standard (linear) extrapolation of the absorption coefficient for very high temperatures in a $\log(\epsilon)$ vs $1/T$ plot does not work very well in this case. On the basis of the low temperature data alone one would determine $\epsilon(T = 1500 \text{ K})$, which is close to the temperature of the molecules after excitation at $1.7 \mu\text{m}$, to be nearly about 1 order of magnitude smaller than measured in this study. It is also obvious that the energy dependence of $\epsilon(\langle E \rangle)$ is strongly determined by the temperature dependence of the absorption coefficient $\epsilon(T)$.

B. Experimental Results. In the present experiments CH₂I₂ was excited with near-IR femtosecond-laser pulses (60 fs) in the $2\nu_1, \nu_2 + \nu_6$ and $\nu_1 + \nu_8/\nu_5 + \nu_6$ spectral region at $1.7 \mu\text{m}$,

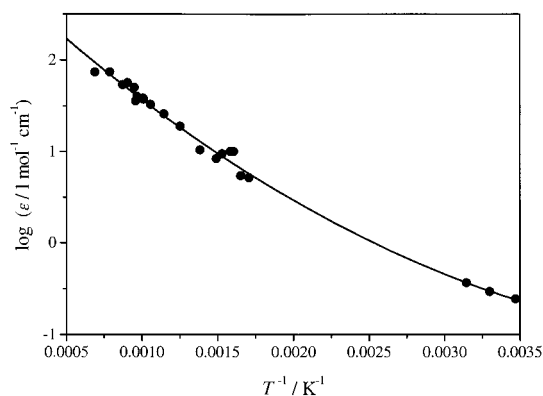


Figure 3. Plot of the logarithm of the absorption coefficient $\log(\epsilon(T))$ at 400 nm as a function of $1/T$. Note that the plot does not show a constant slope. The solid line is a polynomial fit to the data.

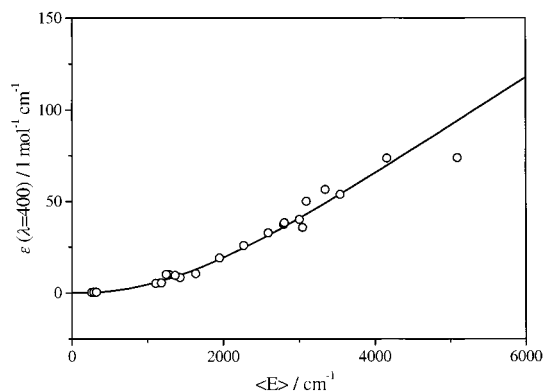


Figure 4. Dependence of $\epsilon(\langle E \rangle)$ on the internal vibrational energy $\langle E \rangle$. For more details see the text. The solid line is a polynomial fit to the data.

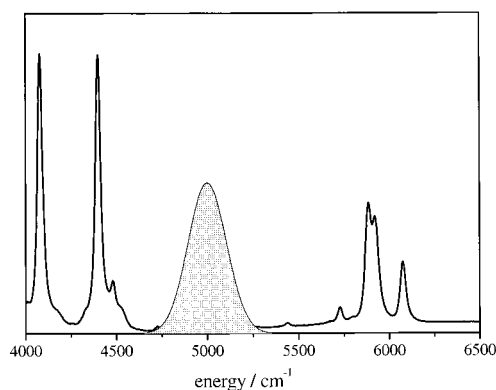


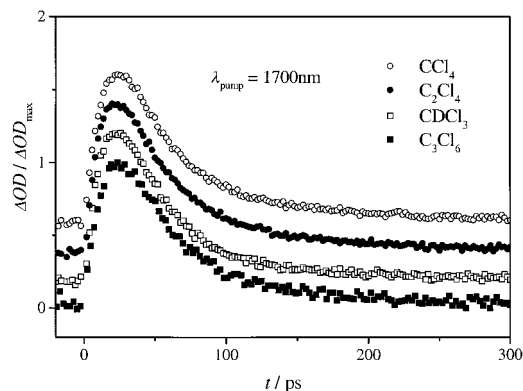
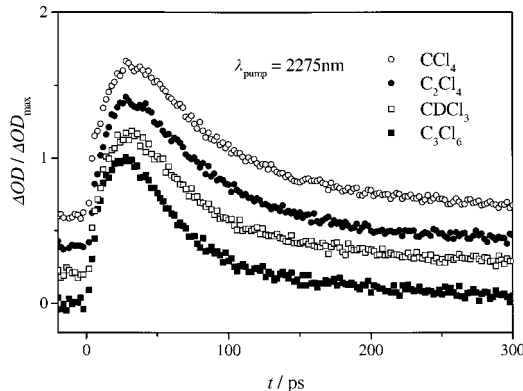
Figure 5. Near-IR spectrum of CH₂I₂ in CCl₄. The spectral widths of the IR excitation pulse is indicated. For details and assignments see the text.

$2.275 \mu\text{m}$, and $2.450 \mu\text{m}$, respectively. In the region of $\nu_{\text{C-H}} = 2$, there are actually 3 bands ($2\nu_1$, $2\nu_6$, and $\nu_1 + \nu_6$) which are all within the bandwidth of the excitation laser pulse. The largest intensity in this region is, however, attributed to $2\nu_1$. Figure 5 shows the IR spectrum of CH₂I₂ in CCl₄ and the spectral width of the excitation pulse. Vibrational assignments have been made on the basis of the frequencies from ref 47 tabulated in Table 1. Note, in the gas phase the strongest IR feature in the $\nu_{\text{C-H}} = 1$ region at 3075 cm^{-1} belongs to ν_6 ; however, we assign the strongest feature in the $\nu_{\text{C-H}} = 2$ region in solution to $2\nu_1$. The weaker feature at higher energies in Figure 5 is assigned to $2\nu_6$ ($\nu_1 + \nu_6$). In various solvents (CCl₄, CDCl₃, C₂Cl₄, C₃Cl₆) the excitation laser has been tuned to the corresponding spectral features. The spectral shift of the absorption bands in the

TABLE 1: Character, Symmetry, and Energies of the Normal Modes of CH₂I₂

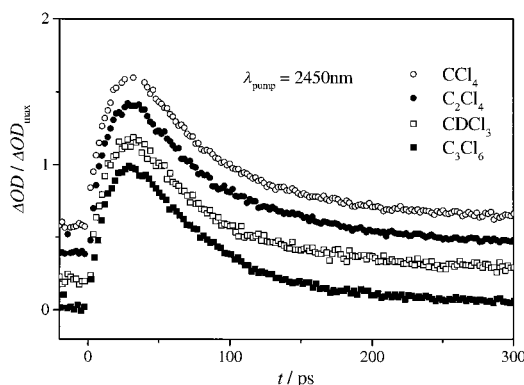
| vibration | character | energy ^{a,b} [cm ⁻¹] | symmetry ^c |
|----------------|---------------------------|---|-----------------------|
| v ₁ | CH ₂ s stretch | 2968 | A ₁ |
| v ₂ | CH ₂ scissor | 1351 | A ₁ |
| v ₃ | CI ₂ s stretch | 486 | A ₁ |
| v ₄ | CI ₂ scissor | 121 | A ₁ |
| v ₅ | CH ₂ twist | 1028 | A ₂ |
| v ₆ | CH ₂ a stretch | 3049 | B ₁ |
| v ₇ | CH ₂ rock | 716 | B ₁ |
| v ₈ | CH ₂ wag | 1105 | B ₂ |
| v ₉ | CI ₂ a stretch | 570 | B ₂ |

^a Kwok et al. *J. Chem. Phys.* **1996**, *104*, 2529. ^b Energies are given for isolated molecules. ^c For C_{2v} point group.

**Figure 6.** Typical time-resolved experimental traces following the IR excitation at 1.70 μm monitoring the solvent dependence of the transient absorption at 400 nm ($\Delta\text{OD}/\Delta\text{OD}_{\text{max}}$ vs time) for different solvents are displayed.**Figure 7.** Typical time-resolved experimental traces following the IR excitation at 2.275 μm monitoring the solvent dependence of the transient absorption at 400 nm ($\Delta\text{OD}/\Delta\text{OD}_{\text{max}}$ vs time) for different solvents are displayed.

different solvents was small, in general, and almost negligible compared to the width of the excitation pulse.

The measured signals, in general, have the following features: The amplitude of the signals (ΔOD) at $t = 0$ is zero but increases at short times (without any recurrences) due to vibrational energy flow into FC-active vibrations until a maximum is reached. The increase of absorption is followed by a subsequent decay of the absorption on a 100–300 ps time scale. In Figures 6–8 typical traces monitoring the excitation wavelength and solvent dependence of the transient absorption at 400 nm following the IR excitation is displayed. It should be noted that the transients we observe critically depend on the wavelength of the excitation laser. It has been verified in all cases that no signal is observed if the excitation laser is off-

**Figure 8.** Typical time-resolved experimental traces following the IR excitation at 2.450 μm monitoring the solvent dependence of the transient absorption at 400 nm ($\Delta\text{OD}/\Delta\text{OD}_{\text{max}}$ vs time) for different solvents are displayed.

resonance (see Figure 5). This shows that the IR excitation initiates the transient response we observe.

C. Data Analysis. The simplest analysis of the obtained signals identifies the rise in the signal with intramolecular vibrational energy equilibration and the decay of the signal with intermolecular energy transfer to the solvent. Since the time scales for the rise and the fall appear to be well separated it is reasonable to assume that the overall “relaxation” consists of two consecutive first-order processes. Although, at first sight, the present model resembles the model of connected heat baths in ref 37, we want to emphasize that, here, we argue in terms of microcanonical ensembles and a relaxation of energy and not in terms of a canonical ensemble and a relaxation of temperature! For the conversion of transient absorption into internal energies we use the temperature-dependent spectra of CH₂I₂ and the dependence of the absorption coefficient on internal energy $\langle E \rangle$ measured in solution and in shock-wave experiments between 275 and 1450 K. This approach resembles the well-established approach of our group to process UV absorption time profiles to obtain VET rates and average energies $\langle \Delta E \rangle$ transferred in collisions in the gas phase (see ref 50 and references therein) and in solution.¹³ We want to emphasize, however, that this approach has not been established for the probe of intramolecular vibrational energy redistribution yet. Therefore, in the following we introduce the concept and discuss why such an approach works for a quantitative evaluation of IVR in CH₂I₂ and other similar molecules.

In our (simplified) picture outline above we consider IVR and VET to be consecutive first-order processes with global (average) time constants τ_{IVR} and τ_{VET} , respectively.

$$E_{\text{“localized”}} \xrightarrow{\tau_{\text{IVR}}} E_{\text{redistributed}} \xrightarrow{\tau_{\text{VET}}} E_{\text{VET}} \quad (1)$$

The physical picture behind this simple model is that the excitation step initially prepares a wave packet and excites a non stationary zeroth order state in which the energy is “localized” at $t = 0$. We will call this energy the localized energy $E_{\text{“localized”}}$, which is roughly the photon energy of the excitation wavelength. We cannot detect the energy $E_{\text{“localized”}}$ directly because the initially excited modes are not FC-active. After some time the energy is delocalized and redistributed and a quasi microcanonical ensemble with an energy $E_{\text{redistributed}}$ is established, which we can measure. It is obvious that $E_{\text{redistributed}}$ depends on time. The phenomenological time constant for this first “relaxation” is τ_{IVR} . Although, the energy of the molecule in this relaxation step (if VET does not take place) is conserved,

IVR may be characterized and followed by a change in the Pauli-entropy of the molecule defined in terms of the population of the states.⁵¹ The second relaxation step is the energy loss due to VET to the solvent with an overall time constant τ_{VET} . Since the initial relaxation step is much faster than the second and since VET is largest for low frequency modes of the molecule we make the reasonable approximation that no VET takes place from the initially excited bond. The expression for the internal energy $E_{\text{redistributed}}$ of the system, which we can measure, can then be written as

$$E_{\text{redistributed}}(t) = E_0 \left[\frac{1/\tau_{\text{rise}}}{1/\tau_{\text{rise}} - 1/\tau_{\text{fall}}} \right] (\exp(-t/\tau_{\text{fall}}) - \exp(-t/\tau_{\text{rise}})) \quad (2)$$

where E_0 is the photon energy ($h\nu_{\text{IR}}$) of the excitation laser. For $\tau_{\text{fall}} \gg \tau_{\text{rise}}$ the expression reduces to

$$E_{\text{redistributed}}(t) = E_0 (\exp(-t/\tau_{\text{fall}}) - \exp(-t/\tau_{\text{rise}})) \quad (2a)$$

Here, we assign τ_{rise} and τ_{fall} to τ_{IVR} and τ_{VET} , respectively. Note, there is no problem in identifying τ_{IVR} and τ_{VET} because τ_{fall} and therefore τ_{VET} can be obtained from a single-exponential fit of the slow decay of the time profiles beyond 25 ps.

The energy $\langle E \rangle$ of the probed subset of states (in state space) of the molecule (which we call the “bath”) is the sum of $E_{\text{redistributed}}$ and the thermal energy at 300 K. Since the transient absorption reflects the enhancement of the cross sections for the electronic transition by vibrational excitation an absorption time profile is then calculated from $E_{\text{redistributed}}(t)$, $\epsilon(\langle E \rangle)$ and eq 3.

$$\Delta\text{OD} \propto \epsilon(\langle E \rangle(t), \lambda = 400) - \epsilon(\langle E \rangle_{298}, \lambda = 400) \quad (3)$$

Throughout this work eq 2 and eq 3 in combination with $\epsilon(\langle E \rangle)$ (Figure 4) has been used to fit the experimental traces. We want to emphasize that this model has only two adjustable parameters τ_{fall} and τ_{rise} which have to be fitted to the experimental traces, in contrast to a recently proposed model.³⁷ With this model we have simulated all experimental traces for all solvents and excitation wavelengths of this study. The results of this simulation procedure are shown in Figures 9–11. The agreement between the experiment and the simulation using the model described above is good, in general. The effective rate constants for IVR and VET for different excitation wavelengths and solvents which have been obtained using the simple model are given in Table 2.

IV. Discussion

A. Is a Simple Model Justified? In Section III we have introduced a simple model from which we can obtain global time constants for IVR and vibrational energy transfer to the solvent. The model proposed and used in the present study may be a crude approximation for a complex IVR process and a VET cascade of CH₂I₂ in solution. However, since the VET of the high-frequency mode excited by the laser is expected to be small^{3–8,11,12} and since IVR is dominated by sequential energy flow between tiers of states with hierarchic couplings and time scales the assumption of fast IVR before VET and the consideration of only one “effective” time constant for intramolecular energy flow is not unreasonable.^{52–54} The single time constant in our model very likely reflects the rate-determining step in a cascade of intramolecular transitions. We want to emphasize here again, that because our pump and probe scheme

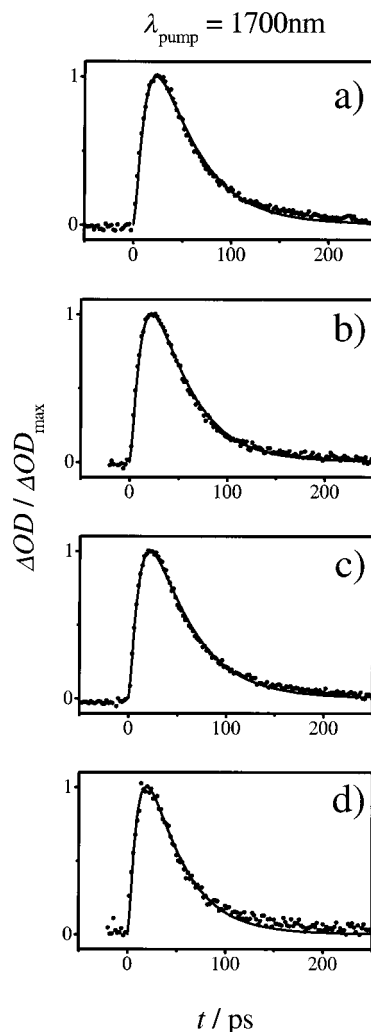


Figure 9. Experimental results (●) for the excitation of CH₂I₂ at 1700 nm for various solvents (a) CCl₄, (b) CDCl₃, (c) C₂Cl₄, and (d) C₃Cl₆, and results from a simulation (—) using the simple model described in the text. For assignments and more details see the text.

is only sensitive to FC-active modes in the molecules we are not able to observe possible intermediates directly.⁴⁰ Also, the assumption of a single exponential decay of the internal energy in VET often works reasonably well.^{4,5,9,11,13,20} However, if needed it is always possible to improve the model by considering multiple step IVR and introducing a VET cascade in the model. For empirical models based on the relaxation of temperature this is quite difficult, and a correlation between experimental observables and microscopic molecular dynamics is often hardly possible.³⁷

As outlined above we use measured spectra in shock waves. It is well documented that the use of high-temperature gas-phase spectra works well for VET in the gas and the condensed phases.^{13,50} However, this is the first time that this technique has been employed for the probe of intramolecular vibrational energy redistribution in solution. Therefore, we need to discuss the implications of such an approach and why this technique works well for a quantitative evaluation of IVR in our case.

Our model implicitly assumes that we probe the internal energy of the equilibrated “bath of states” of the molecule (in solution) which is not excited initially. A simple rate constant describes the process of energy redistribution from the initially excited degrees of freedom to the bath of states which are assumed to be populated nearly statistically (microcanonical ensemble at energy $\langle E \rangle$). Since canonical and microcanonical

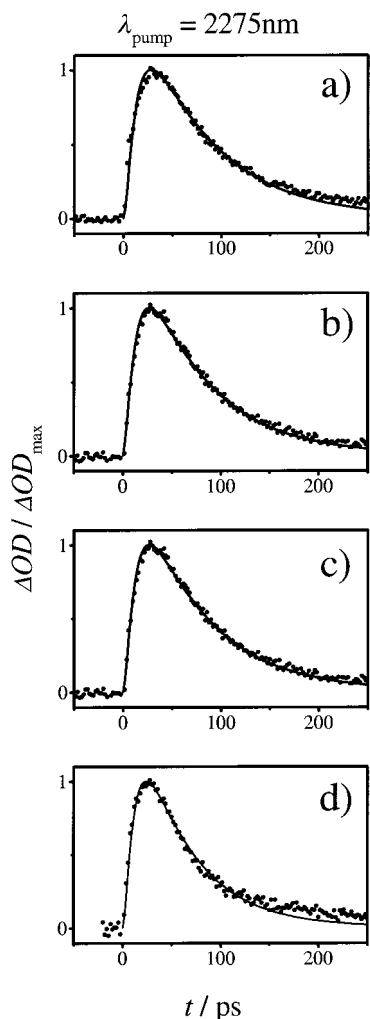


Figure 10. Experimental results (●) for the excitation of CH_2I_2 at 2275 nm for various solvents (a) CCl_4 , (b) CDCl_3 , (c) C_2Cl_4 and (d) C_3Cl_6 and results from a simulation (—) using the simple model described in the text. For assignments and more details see the text.

spectra of molecules with the same average energy $\langle E \rangle$ are identical, we can probe the energy in the equilibrated bath. One may ask whether the degrees of freedom we probe are representative for the energy content in the bath. We have calculated state densities for CH_2I_2 as a function of energy employing a Whitten-Rabinovich procedure. It can easily be shown, that the great majority of all states at the excitation energies are states belonging to combination vibrations of C–I (symmetric and asymmetric) stretch or I–C–I bend, which we probe but which are not excited initially. Because (in general) UV spectra depend only on the population of a few (representative) FC-active modes of the molecule and since we have actually calibrated our absorption, the degrees of freedom we probe in the experiment are surely representative for the distributed energy in all modes of the molecule. This is the reason why it can be used for probing the degree of energy redistribution in the molecule and progress in the evolution of an initially excited nonstationary state (with no excitation in FC-active modes) toward microcanonical equilibrium. The assumption of nearly equilibrated degrees of freedom in the probed bath at all times (due to IVR and collisions) is an approximation in this model. It should be noted, however, that even if IVR does not produce totally equilibrated intermediate “bath states” at short times the model should still provide effective time constants for IVR because we know the initial

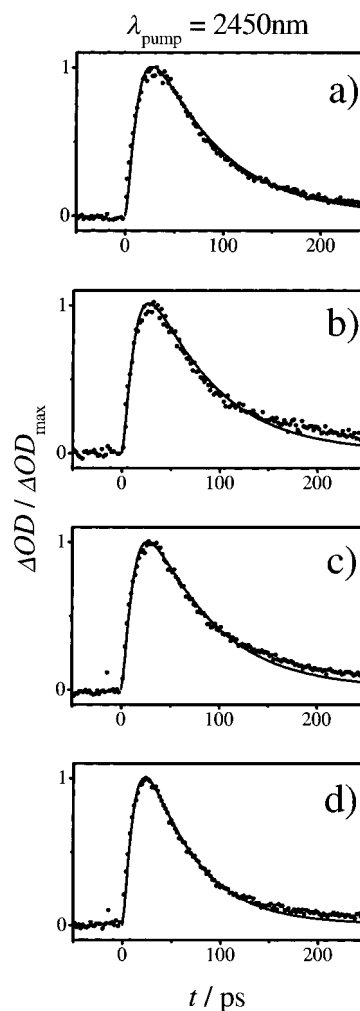


Figure 11. Experimental results (●) for the excitation of CH_2I_2 at 2450 nm for various solvents (a) CCl_4 , (b) CDCl_3 , (c) C_2Cl_4 and (d) C_3Cl_6 and results from a simulation (—) using the simple model described in the text. For assignments and more details see the text.

and final distribution of the molecule which is a strongly non equilibrium distribution at $t = 0$ (with no absorption) and very likely a microcanonical energy distribution (due to IVR and collisions) for longer times (giving rise to the absorption we calibrated). In such a case a single exponential (fitting the observed transient absorption) would just mediate between the two limiting cases, however, it would still be a global measure for IVR. Mechanisms of IVR or IVR pathways can, of course, not be derived from the present approach which only provides one effective rate constant.

B. Intramolecular Vibrational Energy Redistribution (IVR) and Its Energy and Mode Dependence. The experimental findings in the present study are that intramolecular vibrational energy transfer does not change significantly in the solvents we used and the modes we excited (see Table 2). These findings may be due to the small number of modes excited and the similarity of the solvents. It may also be possible that the IVR time constants are accidentally equal. However, before we discuss the present findings we have to ask the question: what is expected? Unfortunately, there exists only a limited number of studies of IVR in solution (see ref 2 and citations therein), such that it is difficult to draw general conclusions about what to expect. On the other hand there exist a large number of studies on IVR both in the frequency and time domain for isolated molecules.^{52,53,55} Taking into account the weakly interacting solute with the solvent we may anticipate that mechanisms found

TABLE 2: Best Fit Parameters τ_{rise} and τ_{fall} ^a for the Simple Kinetic Model for the Simulation of the Transient Absorption Time Profiles for Different Excitation Wavelengths and Solvents^b

| solvent | τ_{rise} /ps | τ_{fall} /ps |
|-----------------------------------|--------------------------|--------------------------|
| $\lambda_{\text{pump}} = 1700$ nm | | |
| CDCl ₃ | 10(±1) | 63(±8) |
| CCl ₄ | 10(±1) | 70(±8) |
| C ₂ Cl ₄ | 9(±1) | 71(±8) |
| C ₃ Cl ₆ | 8(±1) | 62(±8) |
| $\lambda_{\text{pump}} = 2275$ nm | | |
| CDCl ₃ | 11(±1) | 110(±8) |
| CCl ₄ | 11(±1) | 120(±8) |
| C ₂ Cl ₄ | 11(±1) | 110(±8) |
| C ₃ Cl ₆ | 9(±1) | 95(±8) |
| $\lambda_{\text{pump}} = 2450$ nm | | |
| CDCl ₃ | 10(±1) | 115(±8) |
| CCl ₄ | 10(±1) | 117(±8) |
| C ₂ Cl ₄ | 10(±1) | 115(±8) |
| C ₃ Cl ₆ | 9(±1) | 88(±8) |

^a Throughout this work we attribute τ_{rise} and τ_{fall} to intramolecular vibrational energy redistribution and intermolecular energy transfer, respectively. ^b The uncertainty of the parameters in our simple model has been estimated by varying a single parameter, holding the other parameters fixed without significantly degrading the agreement between experiment and the simulation. Since the decay is actually slightly multiexponential, which cannot be fully accounted for with the present simple model, τ_{fall} is actually an average decay constant (for the components) of the overall decay. See the text for more details.

for isolated molecules may also be important in solution. Investigations from the Lehmann/Scoles and Nesbitt groups have focused on the time scales, the energy dependence, and mechanisms of a large number of acetylene homologues.^{55–58} They have found that for large state densities IVR may become independent of the initial excitation energy, the phase space, and the structure of the molecule. In nearly all cases IVR was not correlated with the total density of states of the system⁵⁵ which may be regarded as direct evidence for selective non statistical IVR. In such a case IVR depends only on specific couplings and the local environment of the initially excited mode.^{53,55} For CH₂I₂ we find a state density in the energy range 4000–6000 cm^{−1} between 3 and 16 states/cm^{−1} (total vibrational state density). Using a simple golden rule argument one may be tempted to correlate the IVR time scales simply with the total density of states of the solute molecule in the particular energy regions, an approach which turned out to be unsuccessful in our case. This may be direct evidence for the fact that the rate of intramolecular energy transfer in our case is still dominated by specific low order interactions with only a few near-resonant combination modes and may critically depend on the matrix elements of the anharmonic interaction and the energy gap between the excited mode and the combination mode.⁵³ In this case the IVR should depend strongly on the initial level of excitation. If we inspect the rather similar rates for IVR for different modes we would—at first glance—come to the opposite conclusion. Moreover, excitation in combination bands should lead to faster IVR, because, in general, they are expected to be stronger coupled to background states than the pure overtones. However, Lehmann et al.⁵⁵ have discussed recently that intramolecular coupling is not necessarily stronger in a combination band. For HOOH^{59,60} and propyne^{61–63} distributing the excitation energy in two vibrations (combination band) resulted in slower IVR compared to placing all the energy in one of the O–H or C–H bond stretches. Obviously, the total anharmonicity of the excitation, which is less for a combination band than for a pure overtone of similar energy, may play a

TABLE 3: Mode and Energy Dependence of Time Constants for IVR and VET Obtained in Different Experiments^a

| assignment | energy [cm ^{−1}] | τ_{IVR} [ps] | τ_{VET} [ps] | solvent | ref |
|---------------------------------|----------------------------|--------------------------|--------------------------|------------------|-----------|
| ν_1 | 2960 | 46(±3) | 80(±5) | CCl ₄ | ref 25 |
| $\nu_1 + \nu_8 / \nu_5 + \nu_6$ | 4080 | 10(±1) | 117(±8) | CCl ₄ | this work |
| $\nu_2 + \nu_6$ | 4400 | 10(±1) | 120(±8) | CCl ₄ | this work |
| $2\nu_1$ | 5880 | 10(±1) | 70(±8) | CCl ₄ | this work |
| $2\nu_1$ | 5880 | 10.8(±1.5) | 68(±10) | CCl ₄ | ref 31 |

^a We attribute τ_{rise} and τ_{fall} determined from our simple model in this work to intramolecular vibrational energy redistribution and intermolecular energy transfer, respectively.

significant role in the vibrational dynamics.⁵⁵ From this perspective it may not be surprising that the modes excited in this study exhibit quite similar IVR dynamics (maybe due to accidentally compensating effects).

The comparison of the present data with related data found for other molecules in the gas phase is not as straightforward as it may look at first sight. As stated above, the total state density in the energy range observed is 3–16/cm^{−1}. The vibrational state density available for anharmonic interactions (which would be expected to drive the fast IVR rates observed in this work) is expected to be only one-fourth of this value. At such low vibrational state densities of proper symmetry a dissipative IVR process that can be attributed to the isolated molecule appears unlikely. For example, the homogeneous widths for 10 ps IVR is only 0.52 cm^{−1}. On average, there will be only 1–3 states in this energy range with proper symmetry for anharmonic interactions. This density alone can hardly lead to full dilution of the bright state. From this, one may conclude that the process being observed might be closer to “solvent-induced IVR”. From the gas-phase spectrum we recorded for $\nu_{\text{C–H}} = 2$ it is also not obvious that an extensive fragmentation of the oscillator strength occurs. A comparison with IVR rates in the fundamental range³¹ ($\nu_{\text{C–H}} = 1$) is even more problematic. Clearly this molecule is too small for “isolated molecule” IVR to occur in the fundamentals in the sense of the work reviewed in refs 53 and 55. The decay measured for $\nu_{\text{C–H}} = 1$ could be caused again by some “solvent-induced” process³⁶ which may or may not be the same as the one measured in this work (depending on whether there really is isolated molecule IVR for CH₂I₂ in the first overtone region). An IVR time constant of 40 ps for excitation in $\nu_{\text{C–H}} = 1$ (see Table 3) which was measured in ref 31 may suggest an energy dependence of IVR in this molecule in solution, but since the time constants in the $\nu_{\text{C–H}} = 1$ and $\nu_{\text{C–H}} = 2$ region do not scale with the corresponding density of states we rule out near statistical IVR of CH₂I₂ for the experiments of our present study. The relaxation rates of Bingemann et al.³⁷ for $\nu_{\text{CH}} = 2$ are in agreement with the present data (see Table 3).

It is interesting to note that the IVR time constant for $\nu_{\text{OH}} = 2$ in isolated HONO₂, having a density of states of ~10 states/cm^{−1} in the region of the first OH-overtone has been measured to be on the order of 12 ps.⁴⁶ The similarity of this lifetime for an isolated molecule to those obtained for CH₂I₂ in solution (having almost the same density of states at $\nu_{\text{CH}} = 2$) may suggest that the solvent has only little influence on IVR of CH₂I₂ in the solvents we used.

C. Energy Dependence of Intermolecular Vibrational Energy Transfer. The intermolecular vibrational energy transfer we observe shows that intermolecular vibrational relaxation depends on the nature of the solvent. However, the differences for the solvents used in this study (which are all relatively similar

in nature) are not very large. If we inspect Figures 6–8 and Table 2 the general trends for the solvent dependence of VET are visible, namely, that from CCl_4 to C_2Cl_4 , CDCl_3 and C_3Cl_6 (hexachloropropene) VET becomes slightly faster for all excitation wavelengths. It is known that changing the dipole moment of the solvent, which changes the intermolecular interaction significantly, has a much stronger effect on the VET than changing the internal molecular degrees of freedom of the solvent, as has been observed for the relaxation of CH_2I_2 in deuterated acetone.³¹ Unfortunately, the solubility of the molecule in polar solvents and the fact that we have to avoid solvents with C–H bonds and large absorption in the IR spectral region of interest restricts us to vary the nature of the solvent to a larger extent, i.e., to use other very different protic or aprotic polar solvents. With the present set of solvents we varied the intramolecular degrees of freedom and the density of states of the solvent molecules significantly going from CHCl_3 to C_3Cl_6 but we did only see a small effect in the VET but not anything that is proportional to the density of accepting solvent molecule modes. This seems to indicate that the role of the solvent molecules internal degrees of freedom in solution (state density) is small in general. The reason for this behavior will be given below.

In the Landau-Teller approach the VET rate of a molecule in solution is directly related to the frequency dependent friction $\xi(\omega)$ at the oscillator frequency ω , calculated from the time-correlation function of the solvent forces acting on the vibrational coordinate of the solute.^{2,4–6,9,11,12} $\xi(\omega)$ in general has a maximum at very low frequencies and decays exponentially for increasing ω such that VET is dominated by lowest frequency modes of the solute.^{2,3,11} Therefore, the lower the frequencies and the larger the number of the low frequency modes of the excited molecule the more effective is VET. For a polyatomic solute the relaxation process is characterized by a collisionally induced transition to an internal combination vibration with an energy which usually does not match the initial energy. This energy mismatch must be compensated by the transfer of (vibrational) energy to the continuous low-frequency spectrum of intermolecular degrees of freedom of the solvent.² However, it is well-known that collisions are favored which are characterized by a low order, i.e., only states of the molecule are accessible which differ by a small number of quanta and which excite the least number of quanta in the solvent. It is thus the trade off between a low order process and a small energy gap that is important to have effective VET. As a result of this balance VET is mostly determined by $\xi(\omega)$ at frequencies $\omega > \sim 100 \text{ cm}^{-1}$, i.e., the range beyond the lowest frequency modes describing complex collective motions of the liquid.^{5,64} This is the reason VET rates over wide ranges of density and temperature can often be described in terms of isolated binary collision (IBC) models.^{2,3,9}

Keeping these general considerations in mind we are now able to interpret the experimental observations, i.e., the decays of the transient absorptions. Since in the frequency range of interest $\xi(\omega)$ is determined by the binary solvent–solute interactions (forces) and because these interactions (at least for the family of solvents in this study) do not change significantly, the solvent dependence of the VET rate is not (expected to be) very pronounced. This qualitative argument is supported by recent calculations of the instantaneous normal mode spectrum of CCl_4 and CHCl_3 which have been found to be quite similar.⁶⁵

In the simplest form of our model for the relaxation of energy in CH_2I_2 we assumed that vibrational energy decays exponentially in the molecule with a constant rate with no energy

dependence. This is certainly a crude assumption and provides only overall and average rate constants and in turn a zeroth-order picture of the relaxation. Although, an energy dependence of VET has not been accounted for, the fits of our model to the experimental data are already impressive (see Figures 9–11). However, we have several indications that the overall relaxation is energy dependent. The decays of the internal energy of the molecule inferred from the experimental traces in Figures 6–8 are slightly multiexponential. Although, we model the experimental traces with a single exponential decay reasonably well in Figures 9–11 it is obvious that the modeled decay (and in turn the decay constants) is a compromise between a faster decay at early times and a slower decay at longer times. This is the reason why the modelled traces for longer times in general stay below the experimental time profiles (see Figures 9–11). Since the deviations are small this is not a serious limitation for obtaining overall rate constants. However, it makes a big difference if we want to infer mechanisms of VET, possibly as a function of internal energy $\langle E \rangle$. The overall decays for different excitation wavelengths are different (see Tables 2 and 3). Since the decays and the overall decay constants from the model for excitation in $(\nu_5 + \nu_6)/(\nu_1 + \nu_8)$ and $\nu_2 + \nu_6$ are quite similar but significantly different from excitation in $\nu_{\text{C-H}} = 2$ we conclude that it is not the mode that is excited that dominates the energy transfer but the internal energy and the energy dependence of the VET. It should be noted that, since we have a calibration $\epsilon(\langle E \rangle)$ for the internal energy, we are able to clearly distinguish effects from the energy dependence of the absorption coefficient which may cause absorption time profile to look “multiexponential” as well.

An energy dependence of the VET rate constant for a relatively small molecule like CH_2I_2 in solution is not unexpected.² In contrast, the energy dependence of VET for large molecules has been found to be negligible.^{4,13,20} We identify basically two explanations for the observed weak energy dependence of VET rates which both are related to the lowest frequency modes of the molecule: 1. The energy spacing distribution of these low frequency (combination) modes and their overlap with the frequency dependent friction $\xi(\omega)$ for the solvents under investigation appears to be crucial. 2. Anharmonicity of the lowest frequency modes change the frequency as a function of internal energy and change the overlap with the frequency dependent friction $\xi(\omega)$. The role of anharmonicity in VET is well studied for molecular iodine.² Since the cooling rate is expected to depend sensitively upon this effective frequency change and the overlap with $\xi(\omega)$ the observed effects could also be due to anharmonicity of the lowest frequency modes.

It is interesting to note that for excitation in the fundamental ($\nu_{\text{C-H}} = 1$) of CH_2I_2 the global VET time constant in CCl_4 was measured to be $\tau_{\text{VET}} = 80 \pm 5 \text{ ps}$ (see Table 3) which is between the constants measured in the present study.³¹ These experiments have been performed using single color infrared saturation spectroscopy in which the sample is excited with an intense IR-pump pulse. This leads to a bleaching of the sample if the pumped molecular vibration has an anharmonic progression. The time dependence of the bleaching and thus of the excitation can be monitored by measuring the transmission of a weak IR-probe pulse. The disadvantage of their study is that a calibration of the technique has not been made (or has not been possible) which makes their data difficult to compare with the results from the present study.

In a very recent VET study on CH_2I_2 in solution phenomenological VET constants for $\nu_{\text{C-H}} = 2$ excitation were reported

which are quite similar to the constants we found in this energy region.³⁷ Contrary to our approach they used a simple empirical model in which the temperature rises and decays exponentially. The crucial difference between the two models is that in our model (having two instead of three adjustable parameters) the absorptions have been converted to internal energies and that the energy is assumed to relax instead of the internal temperature of the molecules. Surprisingly, the overall rate constants for $\nu_{\text{C-H}} = 2$ from the study of Bingemann et al.³⁷ are quite similar to ours within experimental error, although, they used a significantly different temperature dependence of the absorption coefficient.

From the argumentation above we conclude that the present data on VET are consistent with a simple model for sequential energy flow with intermolecular energy transfer which can be understood within an isolated binary collision model.^{2,3,6} The observed features of the solvent and energy dependence of VET of CH₂I₂ in solution can all be explained by taking into account the frequency overlap of the low-frequency modes of the molecule or the spectrum of low-frequency combination mode differences at higher excitation energy with the frequency dependent friction $\xi(\omega)$ as well as anharmonicity of the lowest frequencies in the donor molecule. A more sophisticated model for VET would include a master equation with state-to-state rate constants

$$k_{n,n-1} = \frac{2n\xi(\omega)}{\mu\beta\hbar\omega[1 + e^{-\beta\hbar\omega}]} \quad (4)$$

where $\beta = 1/k_{\text{B}}T$. $k_{n,n-1}$ are the rates of transitions of adjacent levels ($n, n - 1$) which satisfy detailed balance.² Such an approach would bridge the gap between microscopic molecular dynamics and our observables.⁶⁴

V. Summary and Conclusions

In conclusion, in this article we used a mode specific experimental approach employing near-infrared and near-ultraviolet femtosecond-laser pulses for the direct measurement of IVR and VET in the liquid phase. This experiment is an extension of a recently published study of the Crim group. In the present work the energy dependence of IVR and VET between 4000 and 6000 cm⁻¹ and the conversion of the absorption data into internal energies are new features. A model based upon the dependence of the electronic absorption on internal energy $\langle E \rangle$ (and temperature) of CH₂I₂ has been used to determine overall times for intramolecular vibrational energy redistribution and intermolecular energy transfer to the solvent. In the simplest version of our model (which we present here) the internal energy of the molecule probed by the population of the FC-active modes rises and decays exponentially on a picosecond (ps) time scale, which reflects the initial intramolecular vibrational energy redistribution and the subsequent energy transfer to the solvent. This zeroth-order approach already described the measured traces well. Overall time constants for IVR have been found to be on the order of 9–10 ps, almost independent of the excitation wavelength, the excited modes and the solvent. In contrast, energy transfer to the solvent takes significantly longer. Overall time constants for VET have been determined in the range between 60 and 120 ps depending on the solvent, the excitation energy but hardly on the mode which was initially excited. These data will provide a stringent benchmark for molecular dynamics calculations which are in progress at present.

Acknowledgment. The authors thank Dr. K. Henning for the measurements of the absorption coefficients at high tem-

peratures in shock waves. Financial support from the Deutsche Forschungsgemeinschaft within the SFB 357 ("Molekulare Mechanismen Unimolekularer Prozesse", A13) and the Fonds der Chemischen Industrie is gratefully acknowledged. Finally, we thank J. Troe, F. F. Crim, and D. Bingemann for interesting and stimulating discussions on this topic.

References and Notes

- (1) Lauberau, A.; Kaiser, W. *Rev. Mod. Phys.* **1978**, *50*, 607.
- (2) Owrutsky, J. C.; Raftery, D.; Hochstrasser, R. M. *Annu. Rev. Phys. Chem.* **1994**, *45*, 519.
- (3) Stratt, R. M.; Maroncelli, M. *J. Phys. Chem.* **1996**, *100*, 12981.
- (4) Heidelberg, C.; Fedchenia, I. I.; Schwarzer, D.; Schroeder, J. *J. Chem. Phys.* **1998**, *108*, 10152.
- (5) Heidelberg, C.; Vikhrenko, V. S.; Schwarzer, D.; Fedchenia, I. I.; Schroeder, J. *J. Chem. Phys.* **1999**, *111*, 8022.
- (6) Oxtoby, D. W. *Adv. Chem. Phys.* **1981**, *47*, 487.
- (7) Oxtoby, D. W. *Annu. Rev. Phys. Chem.* **1981**, *32*, 77.
- (8) Rostkier-Edelstein, D.; Grad, P.; Nitzan, A. *J. Chem. Phys.* **1997**, *107*, 10470.
- (9) Vikhrenko, V. S.; Heidelberg, C.; Schwarzer, D.; Nemtsov, V. B.; Schroeder, J. *J. Chem. Phys.* **1999**, *110*, 5273.
- (10) Velko, S.; Oxtoby, D. W. *J. Chem. Phys.* **1980**, *72*, 2260.
- (11) Egorov, S. A.; Skinner, J. L. *J. Chem. Phys.* **1996**, *105*, 7047.
- (12) Egorov, S. A.; Skinner, J. L. *J. Chem. Phys.* **2000**, *112*, 275.
- (13) Schwarzer, D.; Troe, J.; Zerezke, M. *J. Chem. Phys.* **1997**, *107*, 8380.
- (14) Sukowski, U.; Seilmeier, A.; Elsässer, T.; Fischer, S. F. *J. Chem. Phys.* **1990**, *93*, 4094.
- (15) Schultz, K. E.; Russell, D. J.; Harris, C. B. *J. Chem. Phys.* **1992**, *97*, 5431.
- (16) Gottfried, N. H.; Seilmeier, A.; Kaiser, W. *Chem. Phys. Lett.* **1984**, *111*, 326.
- (17) Sension, R. J.; Szarka, A. Z.; Hochstrasser, R. M. *J. Chem. Phys.* **1992**, *97*, 5239.
- (18) Nakabayashi, T.; Okamoto, H.; Tasumi, M. *J. Phys. Chem. A* **1998**, *102*, 9686.
- (19) Shultz, S. L.; Quian, J.; Jean, J. M. *J. Phys. Chem. A* **1997**, *101*, 1000.
- (20) Nikova, L.; Schwarzer, D.; Troe, J. *Chem. Phys. Lett.* **1995**, *233*, 303.
- (21) Phillips, D. L.; Rodier, J. M.; Myers, A. B. *Chem. Phys.* **1993**, *175*, 1.
- (22) Emmerling, F.; Lettenberg, M.; Lauberau, A. *J. Phys. Chem.* **1996**, *100*, 0, 19251.
- (23) Seilmeier, A.; Scherer, P. O. J.; Kaiser, W. *Chem. Phys. Lett.* **1984**, *105*, 140.
- (24) Laerner, F.; Elsässer, T.; Kaiser, W. *Chem. Phys. Lett.* **1989**, *156*, 381.
- (25) Angel, G.; Gagel, R.; Lauberau, A. *Chem. Phys. Lett.* **1989**, *156*, 169.
- (26) Hubner, H. J.; Wörner, M.; Kaiser, W.; Seilmeier, A. *Chem. Phys. Lett.* **1991**, *182*, 315.
- (27) Seifert, G.; Zürl, R.; Graener, H. *J. Phys. Chem. A* **1999**, *103*, 10749.
- (28) Deak, J. C.; Iwaki, L. K.; Dlott, D. D. *J. Phys. Chem. A* **1998**, *102*, 8193.
- (29) Hartl, I.; Zinth, W. *J. Phys. Chem. A* **2000**, *104*, 4218.
- (30) Lauberau, A.; Kehl, G.; Kaiser, W. *Opt. Commun.* **1974**, *11*, 74.
- (31) Bakker, H. J.; Planken, P. C. M.; Langendijk, A. *J. Chem. Phys.* **1991**, *94*, 6007.
- (32) Woutersen, S.; Emmerichs, U.; Bakker, H. J. *Science* **1997**, *278*, 658.
- (33) Bonn, M.; Brugmans, M. J. P.; Bakker, H. J. *Chem. Phys. Lett.* **1996**, *249*, 81.
- (34) Bakker, H. J.; Planken, P. C. M.; Langendijk, A. *Nature* **1990**, *347*, 745.
- (35) Bakker, H. J.; Planken, P. C. M.; Kuipers, L.; Langendijk, A. *J. Chem. Phys.* **1990**, *94*, 1730.
- (36) Bakker, H. J. *J. Chem. Phys.* **1993**, *98*, 8496.
- (37) Bingemann, D.; King, A.; Crim, F. F. *J. Chem. Phys.* **2000**, *113*, 5018.
- (38) Laenen, R.; Rauscher, C. *Chem. Phys. Lett.* **1997**, *274*, 63.
- (39) Laenen, R.; Simeonidis, K. *Chem. Phys. Lett.* **1999**, *299*, 589.
- (40) Deak, J.; Iwaki, L. K.; Dlott, D. D. *J. Phys. Chem. A* **1999**, *103*, 971.
- (41) Iwaki, L. K.; Deak, J. C.; Rhea, S. T.; Dlott, D. D. *Chem. Phys. Lett.* **1999**, *303*, 176.
- (42) Deak, J. C.; Iwaki, L. K.; Dlott, D. D. *Chem. Phys. Lett.* **1998**, *293*, 405.
- (43) Graener, H.; Lauberau, A. *Appl. Phys. B* **1982**, *29*, 213.

- (44) Häusler, D.; Andresen, P.; Schinke, R. *J. Chem. Phys.* **1987**, *87*, 3949.
- (45) Sinha, A.; Vander Wal, R. L.; Crim, F. F. *J. Chem. Phys.* **1989**, *91*, 2929.
- (46) Bingemann, D.; Gorman, M. P.; King, A. M.; Crim, F. F. *J. Chem. Phys.* **1997**, *107*, 661.
- (47) Kwok, W. M.; Phillips, D. L. *J. Chem. Phys.* **1995**, *104*, 2529.
- (48) Kwok, W. M.; Phillips, D. L. *Chem. Phys. Lett.* **1995**, *235*, 260.
- (49) Quack, M. *Nuovo Cimento* **1981**, *B63*, 358.
- (50) Hippler, H.; Troe, J. In *Advances in Gas-Phase Photochemistry and Kinetics: Bimolecular Collisions*; Ashfold, M. N. R., Baggott, J. E., Eds.; Royal Soc. Chem.: London, 1989.
- (51) Beil, A.; Luckhaus, D.; Quack, M.; Stohner, J. *Ber. Bunsen-Ges. Phys. Chem.* **1997**, *101*, 311.
- (52) Quack, M. *Annu. Rev. Phys. Chem.* **1990**, *41*, 839.
- (53) Nesbitt, D. J.; Field, R. F. *J. Phys. Chem.* **1996**, *100*, 12735.
- (54) Abel, B.; Charvat, A.; Deppe, S. F.; Hamann, H. H. *Ber. Bunsen-Ges. Phys. Chem.* **1997**, *101*, 329.
- (55) Lehmann, K. K.; Scoles, G.; Pate, B. H. *Annu. Rev. Phys. Chem.* **1994**, *45*, 241.
- (56) McIlroy, A.; Nesbitt, D. J. *J. Chem. Phys.* **1989**, *91*, 104.
- (57) Kerstel, E. R. T.; Lehmann, K. K.; Mentel, T. F.; Pate, B. H.; Scoles, G. *J. Phys. Chem.* **1991**, *95*, 8282.
- (58) Gambogi, J. E.; L'Esperance, R. P.; Lehmann, K. K.; Pate, B. H.; Scoles, G. *J. Chem. Phys.* **1992**, *98*, 1116.
- (59) Luo, X.; Rizzo, T. R. *J. Chem. Phys.* **1991**, *94*, 889.
- (60) Luo, X.; Rizzo, T. R. *J. Chem. Phys.* **1992**, *96*, 5129.
- (61) Go, J.; Perry, D. S. *J. Chem. Phys.* **1992**, *97*, 6994.
- (62) Gambogi, J. E.; Timmermanns, J. T.; Lehmann, K. K.; Scoles, G. *J. Chem. Phys.* **1992**, *99*, 9214.
- (63) Gambogi, J.; Kerstel, E. R. T.; Lehmann, K. K.; Scoles, G. *J. Chem. Phys.* **1994**, *100*, 2612.
- (64) Charvat, A.; Aßmann, J.; Abel, B.; Schwarzer, D. Accepted in *Phys. Chem. Chem. Phys.*
- (65) Tokmakoff, A.; Fayer, M. D. *J. Chem. Phys.* **1995**, *103*, 2810.